ELSEVIER

Journal of Molecular Catalysis A: Chemical 171 (2001) 103–114

JOURNAL OF MOLECULAR CATALYSIS A: CHEMICAL

www.elsevier.com/locate/molcata

The adsorption of a series of aromatics in ITQ-1: grand canonical Monte Carlo simulations

Tingjun Hou, Lili Zhu, Xiaojie Xu*

College of Chemistry and Molecular Engineering, Peking University, Beijing 100871, PR China

Received 25 April 2000; accepted 18 January 2001

Abstract

Grand canonical Monte Carlo (GCMC) simulations employing a rigid framework are performed to explore the adsorption behaviors of some aromatics in the purely siliceous MCM-22 zeolite, ITQ-1. Benzene, toluene, *m*-xylene and *o*-xylene are separately simulated at 315 K, investigating a series of pressure from 0.1 to 14 kPa. The potential adsorbed sites of the studied molecules are determined from the mass clouds. The comparison of the different mass clouds indicates that as the kinetic diameters change, the distributions of the adsorbate molecules present regular alterations. The predicted adsorption isotherms of two kinds of adsorbates, including toluene and *m*-xylene are in good agreement with the experimental results. Furthermore, the activation energies of xylenes migrating through the 10-MR windows interconnecting the 12-MR supercages are determined. The energy profiles distinctively suggest that near the 10-MR windows, the potential barrier of *o*-xylene is significantly larger than that of *m*-xylene, which will block the diffusion of *o*-xylene into the interior of the zeolite. The theoretical calculations and experimental results show that at relatively low pressure and temperature, benzene, toluene and *m*-xylene can migrate through the 10-MR windows and reach the adsorption equilibria easily, while *o*-xylene can not overcome the potential barriers along the 12-MR supercages to enter the interior of the zeolite. These results can be well understood by the existence of micropores or cavities of two different sizes: (1) the narrow 10-MR channels, which only benzene and toluene (or smaller molecules) can enter; (2) the wider 12-MR supercages, in which benzene as well as toluene and *m*-xylene can penetrate; (3) the much lower uptake of *o*-xylene or bigger molecules can be ascribed to the difficulty of the entrances of micropores and cavities.

Keywords: ITQ-1; GMC; Molecular adsorption; Aromatics

1. Introduction

Zeolites, as important microporous materials, have been widely used in adsorption and catalytic processes because of their large surface area, confinement, adsorption and molecular sieve properties [1,2]. It is well known that most kinds of zeolites only possess one kind of pore system, for instance, Y and ZSM-5 zeolites. For most catalytic processes, the only one cavity system in some kinds of zeolites may be enough to obtain a good effectiveness. But recently, some applications demonstrate a tendency to employ catalysts involving the simultaneous use of different channel systems. An important example is the combination of Y and ZSM-5 zeolites as catalysts in FCC units to achieve high bottom conversion with high yields on gasoline, propylene and butenes [3].

From the view point of application, it would be of great interest to synthesize structures containing both 12-MR and 10-MR channels in the same

* Corresponding author.
E-mail address: xiaojxu@chem.pku.edu.cn (X. Xu).

1381-1169/01/$ – see front matter
PII: S1381-1169(01)00060-7

zeolite. Recently, a new zeolite named MCM-22 and its applications in many catalytic and adsorption processes have been reported [4,5]. The zeolite has an unusual and unique crystal structure, which has two independent multidimensional channel systems: one pore system being composed of two-dimensional sinusoidal 10-MR channels and the other independent channel system consisting of large 12-MR supercages interconnected with 10-MR windows. The unusual framework topology, high thermal stability, large surface area and good sorption capacity render this kind of zeolite very interesting for catalysis. The studies of the diffusion behaviors of aromatics in MCM-22 are very important, because many separation processes and reactions in MCM-22 are concerned with aromatics. For example, the alkylation of benzene with propylene to produce cumene, the isomerization reaction of dimethyl benzene and the disproportionating reaction of toluene. So the researches of adsorption and localization of aromatics in MCM-22 zeolite will help us to interpret the adsorption and even reaction in the zeolite cavities.

As is well known, the detailed processes of the diffusion or catalytic reaction happening in zeolite framework are somewhat complicated. Some microscopic processes of adsorbates in zeolites are generally difficult or impossible to be determined by experiments. Therefore, it is highly desirable to predict the adsorption and the transport properties of adsorbates from the fundamental knowledge of the structure of a zeolite–adsorbate system. The molecular simulation techniques, including molecular mechanics [6,7], molecular dynamics [8–13] and Monte Carlo simulations [14,15], have been widely used to explore the diffusion processes in the zeolite cavities. By using molecular simulations and molecular graphic techniques, the researchers can visualize and determine the adsorption or diffusion behaviors of reactants and products, even the 'fitting' of the transition state of a given reaction in the available space inside the pores and cavities of zeolites.

In this paper, grand canonical Monte Carlo (GCMC) simulations have been performed to explore the adsorption and localization of a series of aromatics in ITQ-1. First, we calculated the potential distributions and the possible adsorbed sites of a series of aromatics. Second, based on the comparison of the distributions and the adsorption isotherms of the studied molecules, we attempted to characterize the adsorption features of aromatics in ITQ-l.

2. Computer experiments

2.1. ITQ-1 structure

The framework of zeolite MCM-22, which is depicted in Fig. 1, has an interesting and unusual framework topology: two independent pore systems formed by interconnected sinusoidal 10-MR pores of a 4–5.5 Å diameter with an independent 12-MR supercage of 18.2–7.1 Å linked by 10-MR windows. These coexisting pore systems may provide opportunities for a wide variety of catalytic applications in the petrochemical and refining industries. Considering the difficulties of determining Al distribution in disordered zeolites and the high Si/Al ratio of MCM-22 determined by experiments, meanwhile, in order to simplify the simulations, the pure siliceous analogue of MCM-22, ITQ-1, is adopted in this paper. The model of the ITQ-1 is constructed according to the results from the work of Camblor et al. [16]. The zeolite structure is described in *p6/mmm* group with $a = 14.2081$ and $c = 24.9452$ Å.

For purpose of reducing the computations, we make the zeolite atoms fixed at their crystallographic positions. Comparative MD studies with a rigid and a flexible framework model have recently been performed for benzene in ITQ-1 [17]. The simulation results indicate that the intercage diffusion properties of the adsorbates are not significantly influenced by the vibration of zeolite framework. Moreover, the calculation results of different distorted models in the previous work also illustrated that the minor changes of the zeolite framework do not introduce noticeable effects to the simulated results [18].

2.2. Potential parameters

The zeolite and adsorbates are assumed to interact via a pairwise-additive potential between atoms of the adsorbed aromatic molecules and atoms of the zeolites. The site–site interactions are modeled with a Lennard–Jones plus Coulomb potential,

$$V(r_{ij}) = D_{ij}\left\{\left[\frac{(R_0)_{ij}}{R_{ij}}\right]^{12} - 2\left[\frac{(R_0)_{ij}}{R_{ij}}\right]^{6}\right\} + \frac{q_i q_j}{R_{ij}}$$

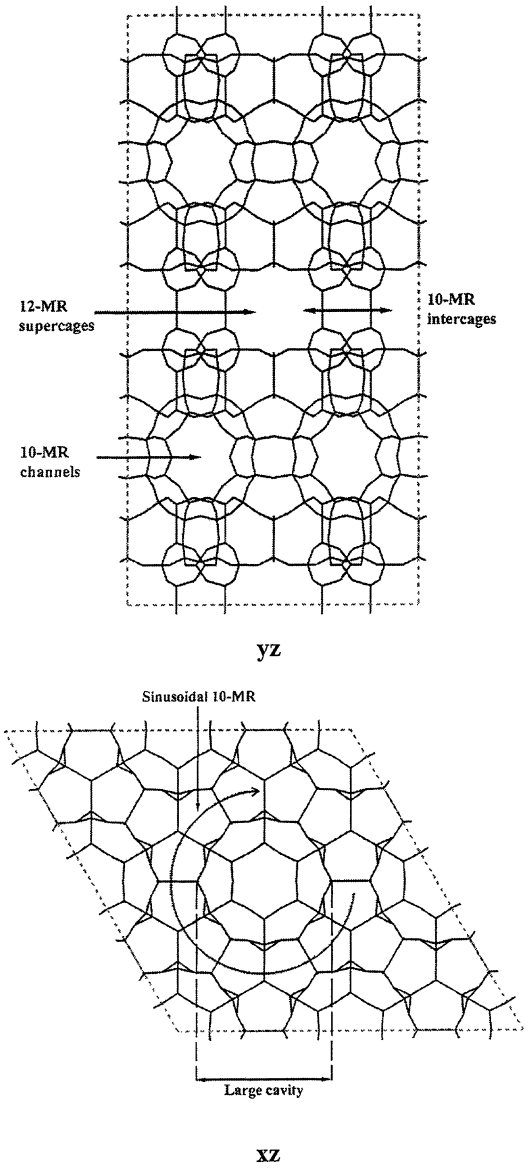

Fig. 1. Schematic view of the independent pore systems in TIQ-1. The sinusoidal 10-MR channels are all interconnected to each other and multiple diffusion trajectories can be allowed to every diffusing molecule. The 12-MR are independent with 10-MR channels which are interconnected through short 10-MR windows.

where i and j indicate atoms of the adsorbate and the zeolite, respectively, and R_{ij} is the distance between them. D_{ij} and $(R_0)_{ij}$ are the Lennard–Jones parameters (Table 1), and q_i and q_j the partial charges on the atoms. The interaction parameters are taken from the Burchart–Dreiding force field. The Burchart force field treats the framework [19], and the Dreiding force field treats the intra- and inter-molecular interactions [20]. The parameters for the framework–molecule interactions are derived from parameters of both force fields, combined with the arithmetic combination rule. This hybrid force field has been tested and distributed in Cerius [21]. The partial charges for O and Si atoms in zeolite framework are taken from the work of Burchart, and those for the atoms in aromatic molecules are computed from AM1 method calculations [22], available in MOPAC 7.0 [23].

Table 1
Lennard–Jones parameter for five types of atoms

Atom type	D_0 (kcal/mol)	R_0 (Å)	q
O_z	0.1648	3.3000	−0.19
Si_z	0.0496	4.2000	+0.38
C_3	0.0951	3.8983	
C_R	0.0951	3.8983	
H	0.0152	3.1950	

2.3. Simulations

GCMC simulation may be the most common technique for predicting the zeolite adsorption phase equilibria from molecular simulations [14,15]. This method simulates the equilibria of a collection of adsorbates in a micropore at constant chemical potential volume, and temperature or pressure. So the GCMC simulation technique enables one to study many important characteristics of adsorbates in zeolite under certain pressure and temperature.

In a GCMC simulation, the initial configuration is generated by one of four moves, for which the acceptance criteria are different. First, a random molecule is picked from the list of adsorbates and is placed in a random position and orientation in the framework. The new configuration is accepted with probability P

$$P = \min\left[1; \exp\left(-\frac{\Delta E}{kT} - \ln\frac{(N_i+1)kT}{f_i V}\right)\right] \qquad (2)$$

where P is the probability of the new configuration being accepted, ΔE the energy change between the new configuration and the previous configuration, k the Boltzmann's constant, T the temperature of the

simulation, N_i the current number of molecules of component i in framework, f_i the fugacity of component i in the gas phase and V the cell volume. Second, a molecule is removed from the framework. The simulation first randomly chooses which adsorbate type to remove, then randomly chooses a molecule of that type in the framework. The new configuration is accepted with probability P

$$P = \min\left[1; \exp\left(-\frac{\Delta E}{kT} + \ln\frac{N_i kT}{f_i V}\right)\right] \quad (3)$$

Third, a adsorbate molecule in the framework is chosen randomly and translated by a random amount within a cube of size 2δ (where δ is the maximum step size). The new configuration is accepted with the probability P

$$P = \min\left[1; \exp\left(-\frac{\Delta E}{kT}\right)\right] \quad (4)$$

In the fourth type of move, a random adsorbate molecule is chosen in the framework. The rotation axis is chosen at random, and the molecule is rotated by a random amount within the range of $-\delta$ to $+\delta$ (where δ is the maximum step size). The new configuration, based on the energy change, is accepted with the same probability applied to the translation move above.

Eight unit cells of zeolite are used to construct the simulation box ($2 \times 2 \times 2$ cells), and periodic boundary conditions are applied in three-dimensions in order to simulate an infinite (macroscopic) system. A cut-off of 10 Å is applied to the Lennard–Jones interactions, and the long-range electrostatic interactions are calculated using the Ewald summation technique [24,25]. First, GCMC calculations are carried out in the condition of standard temperature (315 K) and relatively low pressure (0.2 kPa) to obtain the distribution of aromatics in zeolite framework. Then a series of simulations are performed to predict the adsorption isotherms for the guest molecules at 315 K and 0.0–1.4 kPa pressure.

All calculations are performed in Cerius [21] molecular simulation package on a silicon graphics octane 2-CPU workstation. In order to achieve the real equilibration, the length of the simulations is totally 6×10^6 Monte Carlo steps. Every 600 steps, a configuration of the system is remained. The first 3 million steps are used for equilibration and not included in the averaging.

3. Results and discussion

A deep insight into the channel systems in ITQ-1 reveals some special features which greatly affect the mobility and diffusion behaviors of aromatics in the zeolite lattice (Fig. 1). First, all 10-MR sinusoidal channels interconnect with each other and have high tortuosity. The guest molecules may be restricted through sinusoidal channels in ITQ-1. Second, the 12-MR larger cavities have large dimensions of 7.1 Å × 18.2 Å, and the adsorbate molecules are expected to host and migrate relatively freely. It will be of great interest to investigate their mobility and location inside the cages. Moreover, the 10-MR windows interconnecting 12-MR supercages have relatively small entrance, and high activation energy is needed for relatively large guest molecules migrating through 10-MR windows.

3.1. Distribution of adsorbates in zeolite framework

After 6×10^6 steps of simulations, the equilibration has been achieved, which is indicated by the loading curve and the energy distribution of the simulated system. At 315 K and 0.2 kPa, the mean loading of benzene, toluene, *m*-xylene and *o*-xylene in the simulated box are 57.15, 36.21, 24.14 and 24.00, respectively. Fig. 2 shows the computed histograms of the average adsorbate–zeolite and adsorbate–adsorbate potential experienced by individual molecules at 300 K and 0.2 kPa. The average interaction energies of toluene, *m*-xylene and *o*-xylene with the ITQ-1 zeolite framework are found to be −19.25, −19.74 and −19.76 kcal/mol, respectively. The results indicate that these adsorbates bear similar energetic state in zeolite framework.

The average interaction energy between the benzene and the zeolite (−17.42 kcal/mol) is higher than those between other three kinds of adsorbates and the zeolite. Moreover, its distribution is roughly bimodal, with a maximum around −20.1 kcal/mol and another lower peak around −14.1 kcal/mol. The value at the maximum peak is comparative with those of toluene, *m*-xylene and *o*-xylene with zeolite. The energetic distribution of benzene is much wider than those of other three kinds of adsorbates, which may be determined by the smaller size of benzene. No significant change in the energy distribution is observed when the pressure

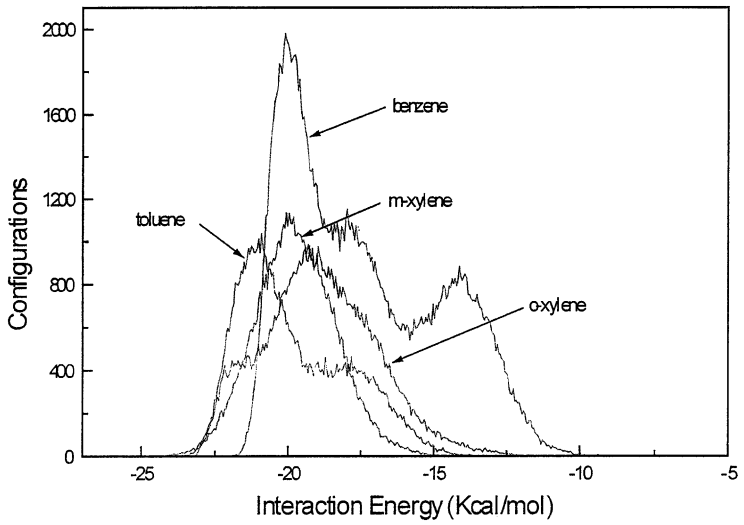

Fig. 2. The average adsorbate–zeolite potential experienced by individual molecules for benzene, toluene, *m*-xylene and *o*-xylene.

increases, which means that the adsorbate molecules remain in the same adsorption sites with the change of the loading.

For the sake of characterizing the siting locations of the adsorbate molecules within the zeolite pores by examining the configurations generated in the GCMC simulations, several mass clouds of benzene are ploted. As a powerful analysis tool, the mass cloud shows the preferred positions of the adsorbate molecules in the zeolite, and the center of mass for each adsorbate in each configuration is displayed as a dot in the model space. All these mass clouds are accumulated over 5000 configurations at 0.2 kPa and 315 K. The mass clouds of benzene, toluene, *m*-xylene and *o*-xylene, with respect to the zeolite framework, are shown in Fig. 3. The results show that the spatial distribution of benzene is roughly territorial, which can be divided into three regions: S1 S2 and S3. S1 site is located at the area of the 10-MR channel intersections, as well as S2 and S3 in 12-MR supercages. From the crystallographic structure of ITQ-1, it has been validated that there exists a high degree of tortuosity in the circular channel. The circular 10-MR channel in ITQ-1 is very small (only 4.0 Å × 5.5 Å), which generates the difficulty of diffusion of benzene through the 10-MR sinusoidal channels of ITQ-1, such as in Fig. 3, so the adsorbate molecules at S1 site are distributed within a very restricted area. A similar conclusion can be drawn from the dynamics simulations in our previous work, in 10-MR sinusoidal channels, the calculated diffusion coefficients are 4.00×10^{-7} cm^2/s (rigid zeolite framework) and 2.06×10^{-7} cm^2/s (flexible zeolite framework), respectively [17]. The present simulations showing the localization of benzene at S1 site agrees with the results from molecular dynamics. From the analyses of the distribution of interaction energies, we find that most of the benzene molecules near S2 site have relatively low interaction energies, and they are concentratively distributed. It is clear that the adsorption behaviors of the benzene at S3 site are quite different, where the adsorbate molecules can be located in a relatively large area. Fig. 2 shows that the distribution of the average interaction energy of benzene with the zeolite is roughly bimodal, and the benzene molecules with interaction energy between −16 and −10 kcal/mol (the smaller peak) are almost located near S3 site. The center part of 12-MR supercage possesses relatively large accommodation space, and the adsorbate molecules can reside in very easily. Moreover, in the 12-MR supercages, the adsorbate molecules are energetically favorable, so the benzene molecules near S3 are considerably delocalized in the vicinity of its preferred sites of adsorption. In Fig. 3a, no benzene molecules are observed in the 10-MR interconnecting region between two 12-MR supercages, which can be suggested by the small entrance of

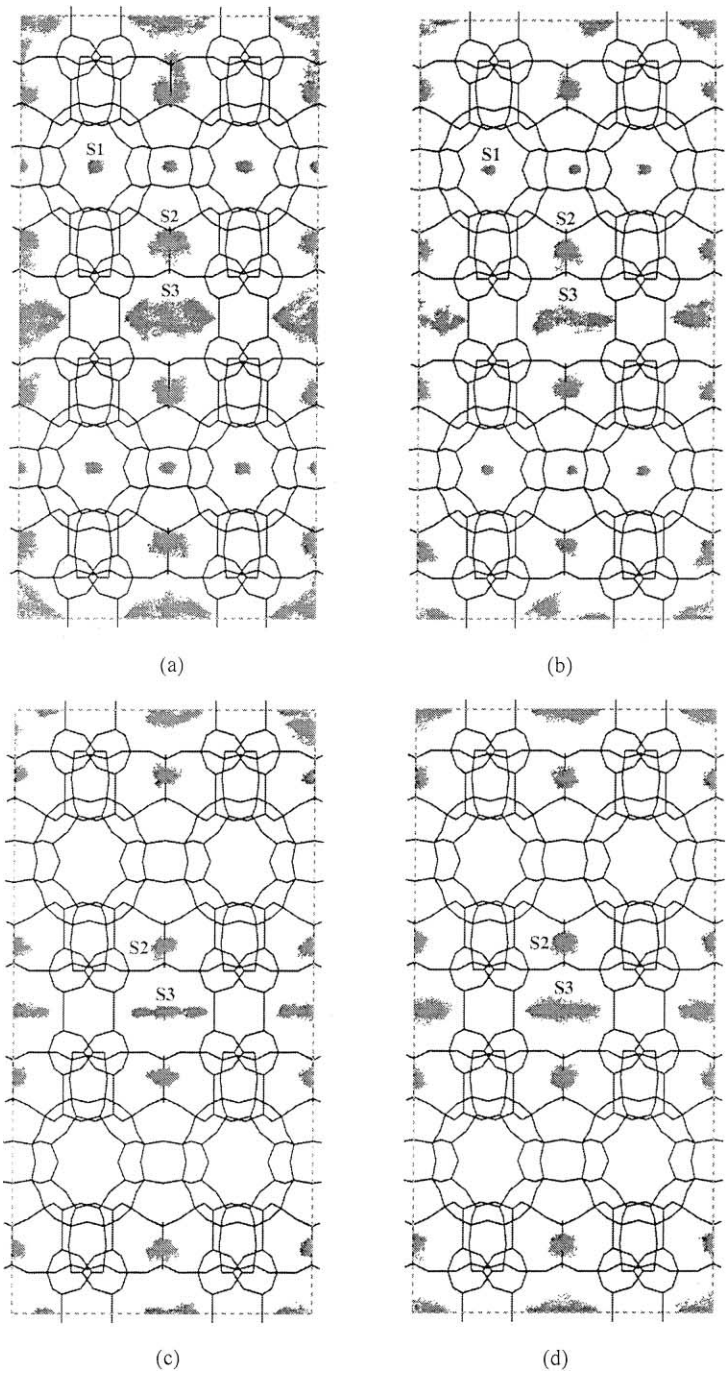

Fig. 3. The mass clouds for four kinds of adsorbates: (a) benzene; (b) toluene; (c) *m*-xylene; (d) *o*-xylene.

the 10-MR interconnecting windows. The benzene molecules near the 10-MR windows are energetically unfavorable.

Comparing Fig. 3a and b, it can be found that the mass clouds of toluene and benzene are quite similar. The only difference is that the distribution of toluene near S1, S2 and S3 sites are restricted to smaller regions, which can be naturally explained by the large molecular size of toluene compared with that of benzene.

The mass clouds of *m*-xylene and *o*-xylene are relatively similar, but they are quite different from those of benzene and toluene. Both of *m*-xylene and *o*-xylene are not observed in 10-MR sinusoidal channels, which can be understood by larger molecular size of these two kinds of molecules. In the small 10-MR channel, enough space can not be afforded to accommodate xylenes. In 12-MR supercages, there are also two adsorbed sites, but the molecular distributions of xylenes at S2 and S3 sites are smaller than those of other two kinds of adsorbates. In Fig. 3c and d, it can be seen that the S2 sites are located nearer to the central part of the 12-MR supercages. These differences among xylenes and benzene can be interpreted by the differences of the molecular size, since the larger adsorbate molecules prefer to hold the positions with larger space.

3.2. The predicted adsorption isotherms

A series of simulations have been performed to get the adsorption isotherms of the studied adsorbate molecules. In order to compare with the experimental results, the simulations are set at 315 K, and at the pressure ranging from 0.0 to 1.4 kPa. The calculated adsorption isotherms of the studied adsorbate molecules are shown in Figs. 4 and 5. From the predicted isotherms, it is evident that the adsorption of the aromatics can happen at very low pressure. When the pressure is below 0.1 kPa, the loadings of the adsorbates increase rapidly from 0 at 0.0 kPa to a certain amount at 0.1 kPa. While the pressure is higher than 0.1 kPa, the increase of loadings is not very rapid. The reason is derived from the favorable interaction between the adsorbate molecules and the zeolite framework, which makes the aromatics possess relatively high loadings at low pressure.

Fig. 2 shows that the four kinds of studied molecules, possess similar average interaction energies, which means that the molecular size will be the major factor influencing the zeolite uptake. Previous experiment of a combined adsorption-microcalorimetric study has been applied to the adsorption–diffusion behaviors of toluene, *m*-xylene and *o*-xylene, and 1,2,4-trimethylbenzene with different kinetic

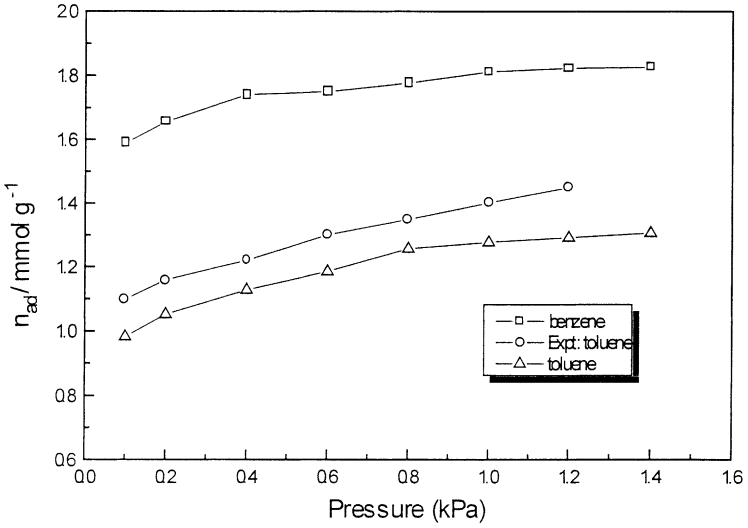

Fig. 4. Simulated adsorption isotherms of benzene, toluene at 315 K and experimental values for toluene.

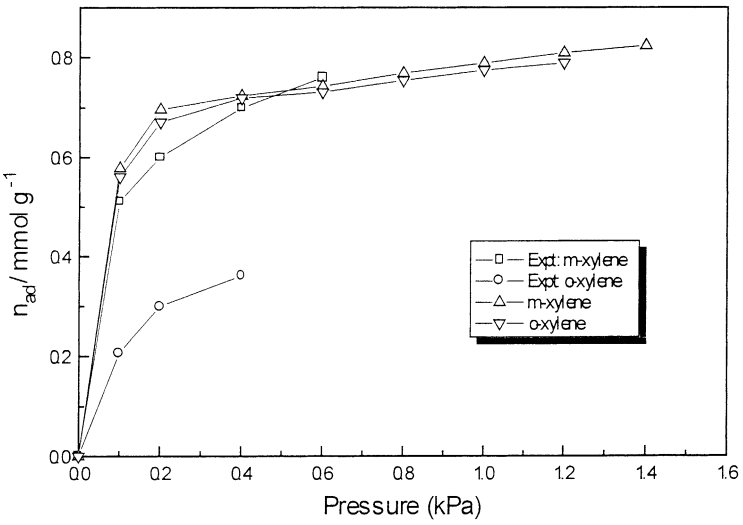

Fig. 5. Simulated and experimental adsorption isotherms of *m*-xylene and *o*-xylene at 315 K.

diameters in MCM-22. The adsorption isotherms have validated that the zeolite update significantly relies on the size of the adsorbate molecules [26]. It is validated that the uptake of *m*-xylene is nearly half the value of toluene. The value for *o*-xylene is much lower and approximately the same as that for 1,2,4-trimethylbenzene. From Fig. 4, it can be seen that the predicted values of toluene are a little lower than those from the experiments. The difference is about 0.1 mmol/g (about 10%). From the overall, the predicted isotherm of toluene is in good agreement with the experimental values. The experimental adsorption isotherm of benzene is unavailable, but the experimental isotherm of toluene can be used as comparison. Only from the viewpoint of molecular size, the benzene is relatively small and its uptake should be higher than that of toluene, which can be well indicated from the predicted isotherm (Fig. 4).

Fig. 5 shows the predicted and experimental isotherms of *m*-xylene and *o*-xylene. It can be noted that the predicted values of *o*-xylene are in excellent agreement with experimental ones, while the predicted values of *o*-xylene are quite different from the experimental measurements. The experimental values show that the loading of *o*-xylene is only about half the value of toluene and approximately the same as that of 1,2,4-trimethylbenzene. In zeolite framework, the *m*-xylene and *o*-xylene experience similar energetic states (Fig. 2). The similar interaction energy can not obviously result in so large differences of amounts of adsorbed *m*-xylene and *o*-xylene. Fig. 1 clearly demonstrates that each supercage is connected to other six supercages through 10-MR windows but in part due to the size and position of the 10-MR interconnecting windows, there may exist some difficulties for large adsorbate molecules migrating through them. Therefore, it can be naturally deduced that the lower uptake of *o*-xylene can be ascribed by the difficulties of *o*-xylene in passing the 10-MR windows. The comparison of *m*-xylene and *o*-xylene shows the kinetic diameter of *o*-xylene is a little larger than that of *m*-xylene. When a *o*-xylene migrates near the 10-MR windows, high activation energy makes it impossible to penetrate into the interior of the zeolite.

In Fig. 5 it is evident that the predicted adsorbed amount of *o*-xylene is overestimated. The GCMC technique adds the adsorbate molecules to the zeolite cavities using the Metropolis criteria, then only tests the final adsorption equilibria of the system. This method does not consider the energetic states of adsorbate along the diffusion pathway. So if there exist some potential barriers while adsorbate diffuses through the channel systems, the adsorbate molecules would not

migrate into the interior cavities of the zeolite and the resulting GCMC calculations may overestimate the adsorbed amounts. Due to the limitation of the entrance of the 10-MR windows, the *o*-xylene apparently can not diffuse into the interior 12-MR supercages in the ITQ-1 zeolite. Consequently, its adsorption capacity is overestimated.

From the dependence of the zeolite uptake on the size of the adsorbate molecules, it can be noted that the existence of microporosity in the range of diameters of these molecules. The uptake of benzene is the highest, and the uptake of *m*-xylene is about half the value of toluene, while is twice that of the *o*-xylene. These results can be well suggested by the existence of micropores or cavities of two different sizes: (1) the narrow 10-MR channels, which only benzene and toluene can enter; (2) wider 12-MR supercages, in which toluene as well as *m*-xylene can penetrate. The much lower uptake of *o*-xylene can be ascribed to adsorption on the entrances of micropores and cavities. In the Sastre's work [27], the author figured out that the benzene intercage motions can be temperature-activated, and when the temperature is increased, intercage diffusion will probably occur, because the interconnecting migration was not observed from his molecular dynamics simulations at 650 K [27]. In Sastre's work [27], through calculating the potential surface of a single benzene molecule following the path connecting two supercage, the energy necessary to across from cage-to-cage is estimated to be about 15 kcal/mol. But from GCMC simulations and previous experimental results, it can be found that at relatively low temperature and pressure, the benzene and toluene can penetrate into the interior cavities through 10-MR windows system relatively freely and achieve adsorption equilibria. So the benzene and toluene intercage motions do not need extra energy from temperature-activation, meanwhile, the potential barriers of benzene, toluene and even *m*-xylene passing through 10-MR windows can be overcome easily. Nevertheless, the factors of probability for benzene, toluene and *m*-xylene through 10-MR windows are relatively low. About 200 ps molecular dynamics in Sastre's work [27] may be too short to obtain the interconnecting migrations of benzene. Consequently, the diffusion coefficient in Sastre's paper is only a rough estimation of intercage diffusion of benzene in 12-MR supercage [27].

3.3. The activation energies of m-xylene and o-xylene through 10-MR windows

From the comparison between the simulated and experimental results of the adsorption isotherms of xylenes, it is obvious that the uptake of these two kinds of molecules is mainly determined by the probability of passing through the 10-MR windows. Certainly, the probability is determined by the activation energies of xylenes through the 10-MR interconnecting cages. For this purpose, a single *m*-xylene or *o*-xylene molecule is forced to follow the path connecting two supercages in the ITQ-1 zeolite. During the calculations, the zeolite structure is rigid, but conformations of the adsorbate molecules are flexible. The potential includes three terms: Lennard–Jones and Coulomb potential between the zeolite and xylenes, plus the internal potential of the adsorbate molecules.

Energy minimizations under constraints are used for the systematic search for local minima. First, we select a simple pathway along the center axis through 12-MR supercages and 10-MR windows. Along the pathway, the xylene molecules are translated and rotated through the supercages. A simple energy minimization strategy is performed to optimize the conformation of the xylenes to find the local potential minima. Then, we divide the corresponding path connecting the local potential minimum positions into small steps of 0.5 Å distance from each other. For all the corresponding conformations, the center-of-mass of the adsorbate molecule is constrained and the interaction energy between the xylene and the zeolite framework is computed after energy minimization.

Figs. 6 and 7 show the minimum guest–host interaction energy as a function of the distance between the center-of-mass of the xylene and the initial position of the guest molecule. In Figs. 6 and 7, there exists a sharp peak, which means there exists an obvious potential barrier when xylene migrates through the 10-MR windows. Fig. 8 shows the critical points (A–E) followed by *o*-xylene as it is pulled from cage-to-cage. The B point corresponds to the peak point B in Fig. 7, which is located near the 10-MR windows. The energy profile of the *o*-xylene as it is pulled from cage-to-cage in the ITQ-1 structure is very similar to that of the *m*-xylene (Figs. 6 and 7), but the value of the peak point in Fig. 6 is quite lower than that in Fig. 7. For *m*-xylene and *o*-xylene, the

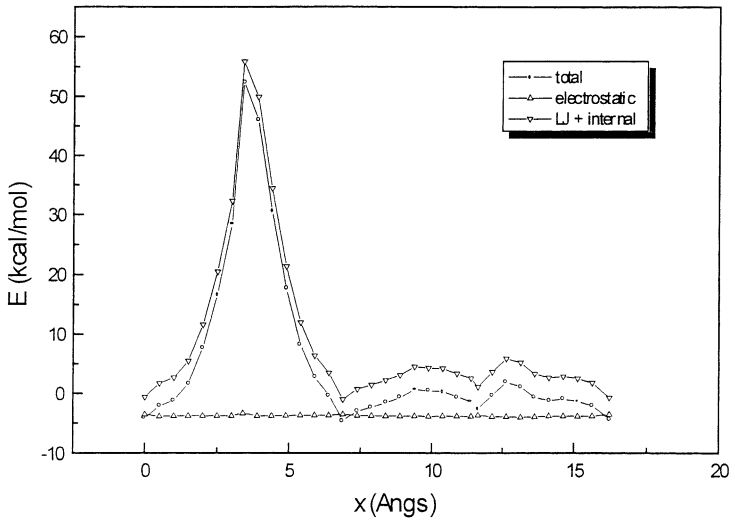

Fig. 6. Energy profile of *m*-xylene in ITQ-l as a function of the distance between the center-of-mass of the molecule and the initial position while it is pulled from cage-to-cage.

estimated energy necessary to cross from cage-to-cage is around 55 and 120 kcal/mol, respectively. The high activation energy of *o*-xylene through the 10-MR interconnecting cages makes this kind of adsorbate molecule impossible to cross the 10-MR windows. It should be noted that in realistic systems, the activation energy for xylene crossing 10-MR windows would be much lower. Because in this paper, the used zeolite framework is rigid, which will result in the overestimation of the Lennard–Jones potential especially while the xylene migrates near the 10-MR windows. Our ultimate goal is not to determine the precise

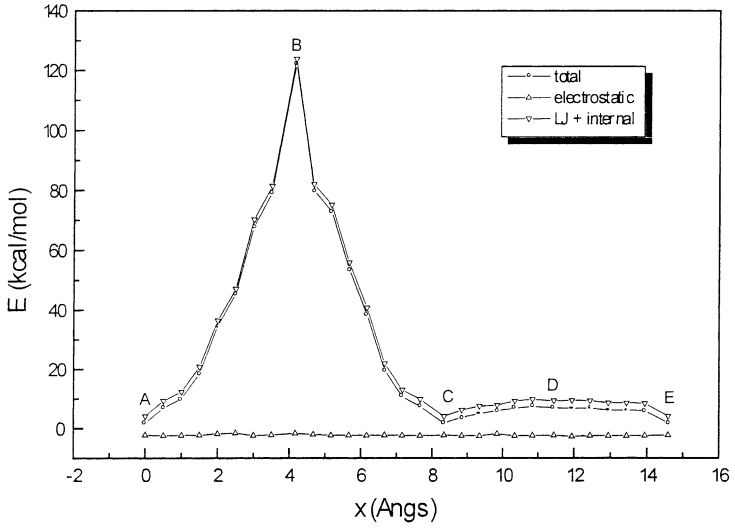

Fig. 7. Energy profile of *o*-xylene in ITQ-l as a function of the distance between the center-of-mass of the molecule and the initial position while it is pulled from cage-to-cage.

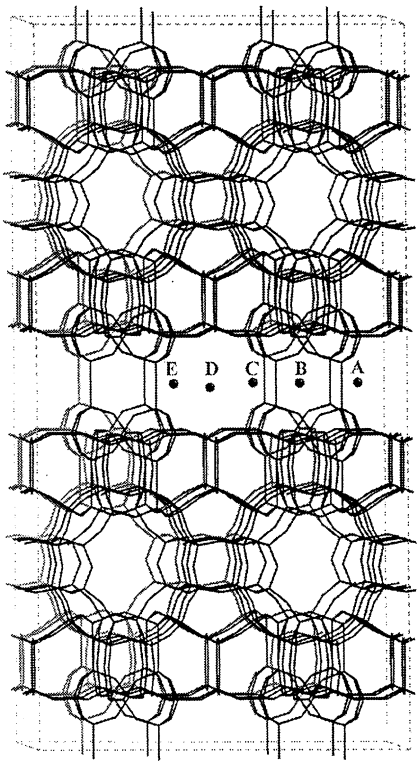

Fig. 8. Side view of the ITQ-1 structure showing the critical points (A–E) followed by *o*-xylene as it is pulled from cage-to-cage.

activation energy of xylene across 10-MR windows, but to semi-quantitatively compare the probability of *m*-xylene and *o*-xylene for the cage-to-cage migration from the energetic level. The simulated results have validated that it is much more difficult for *o*-xylene to cross the 10-MR windows than *m*-xylene.

Moreover, the separate contributions to the activation energy have been computed, too. The first contribution comes from the Lennard–Jones plus the xylene conformational energy, and the second contribution comes from the electrostatic interaction between the xylene and the zeolite structure. In Figs. 6 and 7, between the critical points A and C, the total interaction energy seems to mainly come from the van der Waals potential, and the distribution of electrostatic seems not to be very important. In this region, when xylene migrates near the 10-MR windows, the Lennard–Jones repulsion is quite significant. But between the critical points C and E, both contributions from electrostatic and Lennard–Jones are important.

From the analyses of the structure of *m*-xylene and *o*-xylene, it can be found that their molecular size and shape only exist a little difference. The kinetic diameter of *m*-xylene is a little smaller than that of *o*-xylene but the tiny difference makes the adsorption capacity of the *m*-xylene and *o*-xylene quite different. As a result, the *m*-xylene can penetrate into the interior 12-MR supercage of the zeolite while the *o*-xylene can only be adsorbed on the entrance of micropores and cavities or the surface of the zeolite.

4. Conclusion

Molecular simulations for the adsorption of some aromatics in ITQ-1 zeolite are performed using a grand canonical Monte Carlo technique. The calculated mass clouds clearly demonstrate the potential adsorption sites of the studied molecules and some differences are observed as the change of the kinetic diameters. The simulated adsorption isotherms are systematically compared to available experimental data. At 315 K and 0.1–l.4 kPa, the predicted adsorption values of the pure toluene and *m*-xylene are in good agreement with the experiments. However, the simulated isotherm of the pure *o*-xylene obviously does not agree quantitatively with the experimental data, and the departure comes from the inherent shortcomings of the GCMC technique.

In order to investigate the difference between adsorbed amounts of the *m*-xylene and the *o*-xylene, the activation energies of the cage-to-cage diffusion of xylenes are determined by a simple model only possessing one adsorbate molecule. The predicted energy profiles distinctively suggest that near 10-MR windows, the potential barrier of *o*-xylene is significantly larger than that of *m*-xylene, which will block the diffusion of *o*-xylene into the interior of 12-MR supercages of the zeolite. The regularity of the dependence of the zeolite uptake on the size of the adsorbate molecules can be well interpreted by our simulations and previous experiments.

Acknowledgements

The work is supported by Research Institute of Petrochemical Processing of SINOPEC and NCSF

29992590-2. The authors are indebted to Prof. D.D. Li and Prof. E.Z. Mm of Research Institute of Petrochemical Processing for their very helpful suggestions.

References

[1] N.Y. Chen, T.K. Degnan, C.M. Smith, Molecular Transport and Reaction in Zeolites, VCH Publishers, New York, 1994.
[2] J.A. Rabo, Guidelines to the Mastering of Zeolite Properties, Plenum Press, New York, 1990.
[3] J. Biswas, L.E. Maxwell, Appl. Catal. 58 (1990) 1.
[4] M.E. Leonowicz, J.A. Lawton, S.L. Lawton, M.K. Robin, Science 264 (1994) 1910.
[5] M.K. Rubin, P. Chu, US Patent no. 4954325, 1990.
[6] J.A. Horsley, J.D. Fellmann, E.G. Derouane, C.M. Freeman, J. Catal. 147 (1994) 231.
[7] H. Klein, C. Kirschhock, H. Fuess, J. Phys. Chem. 98 (1994) 12345.
[8] P. Demontis, G.B. Suffritti, A. Alberti, S. Quartieri, E.S. Fois, A. Gamba, Gazz. Chim. Ital. 116 (1986) 459.
[9] S. Yashonath, Chem. Phys. Lett. 177 (1991) 54.
[10] S. Yashonath, P. Demontis, M.L. Klein, J. Phys. Chem. 95 (1991) 5881.
[11] C.R.A. Catlow, C.M. Freeman, B. Vessal, S.M. Tomlinson, M. Leslie, J. Chem. Soc., Faraday Trans. 87 (1991) 1947.
[12] P. Demontis, G.B. Suffritti, E.S. Fois, S. Quartieri, J. Phys. Chem. 96 (1992) 1482.
[13] R.L. June, A.T. Bell, D.N. Theodorou, J. Phys. Chem. 96 (1992) 1051.
[14] Q.S. Randall, T.B. Alexis, N.T. Doros, J. Phys. Chem. 97 (1993) 13742.
[15] P.A. Van Tassl, H. Davis, A.V. Mccormick, J. Chem. Phys. 98 (1993) 4173.
[16] M.A. Camblor, A. Corma, M.J. Diaz-Cabanas, C. Baerlocher, J. Phys. Chem. B 102 (1998) 44.
[17] T.J. Hou, L.L. Zhu, X.J. Xu, J. Phys. Chem. B 104 (2000) 9356.
[18] T.J. Hou, L.L. Zhu, X.J. Xu, J. Mol. Struct. (Theochem.), 535 (2001) 9.
[19] E.D.V. Burchan, Ph.D. Thesis, 1992.
[20] S.L. Mayo, B.D. Olafson, W.A. Goddard, J. Phys. Chem. 94 (1990) 8897.
[21] Cerius User's Guide, Molecular Simulation Inc., 1998.
[22] M.J.S. Dewar, E.G. Zoebisch, E.F. Healy, J.J.P. Stewart, J. Am. Chem. Soc. 107 (1985) 3902.
[23] Mopac version 7.0, Quantum Chemistry Program Exchange, Bloomington, USA, 1995, http.//qcpe.chem.indiana.edu/.
[24] P.P. Ewald, Ann. D. Physik. 64 (1921) 253.
[25] N. Karasawa, W.A. Goddard, J. Phys. Chem. 93 (1989) 7320.
[26] A. Coma, A. Corell, J. Pérez-Pariente, J.M. Guil, R. Guil-López, S. Nicolopoulus, J. Gonzalez-Calbct, M. Vallet-Regi, Zeolite 17 (1996) 7.
[27] G. Sastre, C.R.A. Catlow, A. Corma, J. Phys. Chem. 103 (1999) 5187.